Published by IOP Publishing for Sissa Medialab

Received: *December 6, 2019*
Revised: *February 4, 2020*
Accepted: *February 5, 2020*
Published: *March 20, 2020*

XII International Symposium on Radiation from Relativistic Electrons in Periodic Structures — RREPS-19
September 16–20, 2019
Belgorod, Russian Federation

Theoretical study of the dose measurements reliability with longitudinally arranged dosimetry films in materials with different densities

A. Bulavskaya,[a] Y. Cherepennikov,[a] A. Grigorieva,[a,1] I. Miloichikova,[a,b] Z. Startseva,[b] S. Stuchebrov[a] and V. Velikaya[b]

[a] *National Research Tomsk Polytechnic University, 30 Lenin Avenue, Tomsk, 634050, Russian Federation*
[b] *Cancer Research Institute of Tomsk NRMC, 5 Kooperativny Street, Tomsk, 634009, Russian Federation*

E-mail: agrigorieva@tpu.ru

Abstract: *Investigation purpose.* Theoretical study of the depth dose measurements for therapeutic electron beam with longitudinally arranged dosimetry films in materials with different densities. *Materials and methods.* The work studies how the density of the medium, in which electrons propagate, affects the measured percentage depth dose and its reliability (PDD). For that, we calculate the distribution of the electron beam dose distribution in homogeneous materials with different densities and in a dosimetry film placed in materials with these densities. The density of material in the calculation varies from 0.4 to 2.3 g/cm^3 with a 0.1 g/cm^3 step. The coincidence of the PDD within the experimental measurement accuracy, that equals 4% for dosimetry film and 2% for measurements without it, is chosen as the data fitting criterion. *Results.* The PDD calculated for two geometries and for different media densities is the result of this work. The calculation shows that PDD difference is negligible when the density of the film is equal to the media one. With decreasing of the media density the difference appears in the regions of both shallow and great depth. The PDD is lower for the geometry with film than for geometry without it in case of these densities. When the media density is rising the opposite effect is observed: the PDD in the film is higher than in geometry without film. The maximum range and therapeutic range in both geometries coincide for the calculated curves throughout the range under study. *Discussion.* The work shows applicability of the investigated method for measurement of the electron beam percentage depth dose in media

[1] Corresponding author.

https://doi.org/10.1088/1748-0221/15/03/C03037

with densities ranging from 0.9 to 1.8 g/cm^3. The results show that PDD measurement method with longitudinally arranged dosimetry films can be applied to determine the maximum range and therapeutic range for media with densities of 0.4 to 2.3 g/cm^3, and to measure the half-value depth for media with densities ranging from 0.7 to 2.1 g/cm^3.

Keywords: Accelerator Applications; Models and simulations; Simulation methods and programs

Contents

1 Introduction

Numerical studies in various fields focus on increasing the efficiency of the radiotherapy procedures [1–4]. The use of electron beams in radiation therapy provides good therapeutic results in the treatment of malignant tumors [3–5]. With the requirements for the accuracy of dose delivery becoming more and more stringent, the demand is growing for complex dose fields during radiotherapy sessions [4, 5]. Currently, the dose fields of clinical electron beams are formed using standard sets of blocks and collimators [4].

Electron radiation therapy with conformal fields minimizes the exposure of healthy tissues and, consequently, reduces the negative effects [3–5]. This requires individual radiation fields that can be formed using custom-made collimators [4] produced for each patient by metal melting or cutting [6, 7]. However, metalworking requires trained professionals and well-equipped facilities, which is often hard to arrange in a medical institution.

The papers [8–11] proposes a method of forming clinical electron beams by 3D printed polymer samples. 3D printing provides a fast and accurate way to produce custom-shaped samples specific to particular clinical cases. Being cost-effective and user-friendly, the method will be easy to introduce into medical practice [8–13].

To study the possibility of using plastic for forming electron beams, it is necessary to explore the absorption of electrons in this material. The main experimental parameter to characterize this interaction is the percentage depth dose (PDD).

The PDD can be measured experimentally by a few methods in line with the international recommendations on clinical dosimetry, e.g. TG-51 protocol by Task Group 51 of the Radiation Therapy Committee of the American Association of Physicists in Medicine (AAPM) [14] and TRS-398 protocol by the International Atomic Energy Agency (IAEA) [15]. One method is to measure the dose in a medium at different depths using plates of different thicknesses made of the material under study. The material is also used to produce a custom-shaped plate that can accommodate a

2020 JINST 15 C03037

detector without air gaps. The PDD can be measured at different depths by rearranging the plates. The main drawback of this method is the necessity to perform a separate measurement for each depth. Thus, to measure the PDD of 6 MeV electrons in a tissue-equivalent material with 1 mm accuracy, it is necessary to perform more than 20 measurements. Obviously, this method is time and labor consuming.

Another method of the PDD measurement involves dosimetry films [16, 17]. A well-known drawback of this method is relatively low measurement error, which is about 4% for absolute dosimetry and about 2% for relative one [16, 18, 19]. Nevertheless, this approach is widely used because of a number of advantages. It is time-saving, easy to operate, provides high-resolution and sensitivity to different types of ionizing radiation in a wide energy range, while detecting elements is compact and can be easily placed in different objects [16–21]. The film is placed between two plates made of the material under study with sufficient thickness to account for particle scattering in this material. The plane of the film coincides with the axis of electron propagation. Thus, the sensitive volume of the dosimetry film is located along the propagation of the beam, so one measurement is enough to determine the PDD of electrons in the material. This method is convenient due to its high speed. However, when the PDD is determined in this geometry, the medium under study is supposed to be tissue-equivalent [16, 17]. In reality, the density of many plastics differs much from the 1 g/cm^3, which is a reference value for tissue-equivalent materials. In addition, such approach is widely used for conformal radiotherapy plan verification in heterogeneous phantoms with bones, muscles and fat imitations [22, 23]. Hence, the question arises whether this method is applicable for materials with different densities.

The aim of this work is to estimate the method efficiency for measuring the PDD of a clinical electron beam using longitudinally arranged dosimetry films in tissue nonequivalent materials. We use numerical simulation to calculate the electron beam dose distribution in homogeneous materials with different densities and in a film dosimeter placed in these materials.

2 Methods and materials

2.1 Software for numerical simulation

The Monte Carlo method is used for simulation as one of the most widespread in medical physics investigation [24–27]. In previous research [28] we have shown that the simulating results of the absorbed energy and the electron depth dose distributions in different media obtained using the PCLab software and reference toolkits Geant4 and ITS demonstrate good agreement.

Based on these results the PCLab software [29] is chosen for numerical simulation in this work. This software processes the parameters of the electron beam and the nature of particle interaction with various materials by the Monte Carlo method. The PCLab is created based on the software package EPHCA [30]. It allows to consider the following types of electrons and positrons interactions: elastic and ionizing collisions and bremsstrahlung radiation. The Goudsmit-Saunderson and Moliere distributions describes the electrons and positrons angular deflections at the end of the trajectory. Simulated propagation of the electrons is considered as a cascade process.

2020 JINST 15 C03037

2.2 Radiation source

In the simulation, a flat 10×10 cm^2 parallel electron beam with a uniform distribution was used as a primary radiation source. The average electron energy is 5.3 MeV with a standard deviation of 0.374 MeV. The parameters of the beam correspond to the beam of the medical accelerator ONCOR Impression Plus (Siemens, Oncology Care Systems, Germany) [31].

2.3 Simulated geometry

The simulation is carried out for two geometries, which is shown in figure 1.

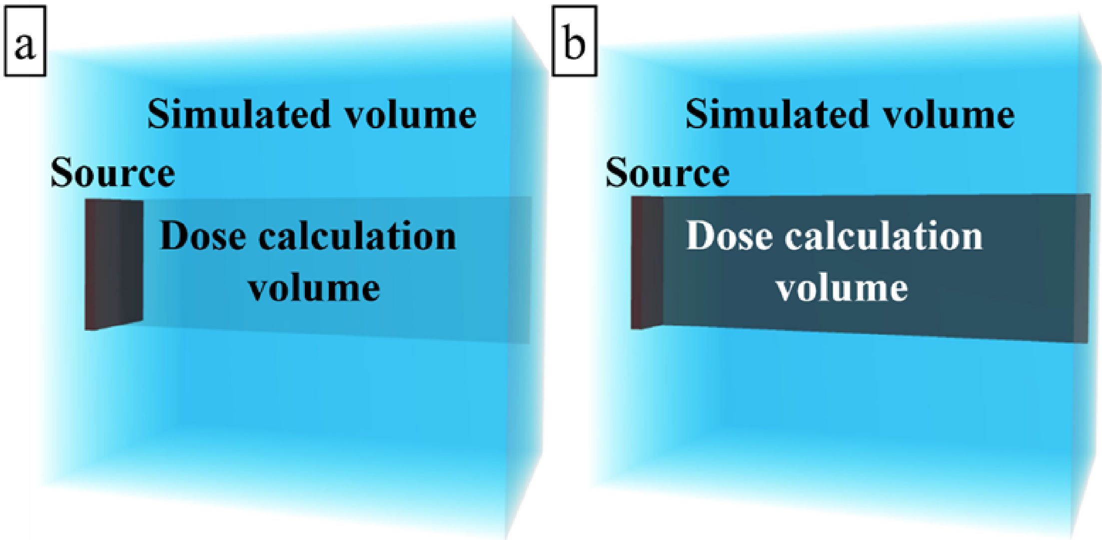

Figure 1. Simulated geometry: a – geometry 1 (without a dosimetry film); b – geometry 2 (with a dosimetry film).

The electron interaction with a target is simulated in a volume with a 20×20 cm^2 square cross section for all geometries. The depth of the simulated volume is chosen in accordance with the materials density to optimize the time of simulation. The dose values are calculated discretely in rectangular 0.3×5.0×1.0 mm^3 volumes and normalized to a maximum. For the first geometry (without a dosimetry film), the PDD is calculated for the investigated material volume with a 10×0.03 cm^2 cross section and throughout its depth. For the second geometry, the same calculated volume is filled by the equivalent of a dosimetry film material.

2.4 Materials under study

To estimate how the density of the material affects the PDD measurement results with dosimetry films, we calculate the PDD in layers of water with different densities. Water is chosen as a common tissue-equivalent material.

The elemental composition of the simulated media remains constant so that the chemical elements of the medium could not interfere with the results. It should be noted that chemical composition of water is close enough to plastics, which can be used for 3D-printing and consist of low Z elements. However, the density of the most common plastics varies from 0.9 g/cm^3 for PP

2020 JINST 15 C03037

(polypropylene) and 1.04 g/cm^3 for ABS (acrylonitrile butadiene styrene) to 1.24 g/cm^3 for PLA (polylactide) and 2.1 g/cm^3 for FPE (flexible polyester) [32]. Considering it, we have chosen the density range for the simulation. This simulation is done for the density range from 0.4 to 2.3 g/cm^3 with a 0.1 g/cm^3 step.

For the second geometry, the PDD is calculated for the equivalent of a dosimetry film. The chemical composition, density, and thickness is chosen according to the technical specification for the Gafchromic EBT3 films [33].

3 Results and discussions

Figure 2 shows the simulated results for several density values. The number of initial electrons histories run is 10^{10} and the error of simulated results is less than 1%. For low media densities, a decline in the PDD is observed in the film at small depth, which is not present in the geometry without a film (figure 2a). With an increase in the density of the medium, this decline becomes less noticeable (figure 2b, 2c), and at equal densities, the difference is not observed (figure 2d). With a further increase in the density, this part of the PDD in the film becomes higher than in the geometry without a film. This difference grows with a decrease in the density (figure 2e, 2f).

In the region of large depths for low densities, the PDD is somewhat lower than for the geometry with a film. This difference also decreases with an increase in the medium density. When the medium density exceeds the film density, the PDD in this region grows higher than in the geometry with a film.

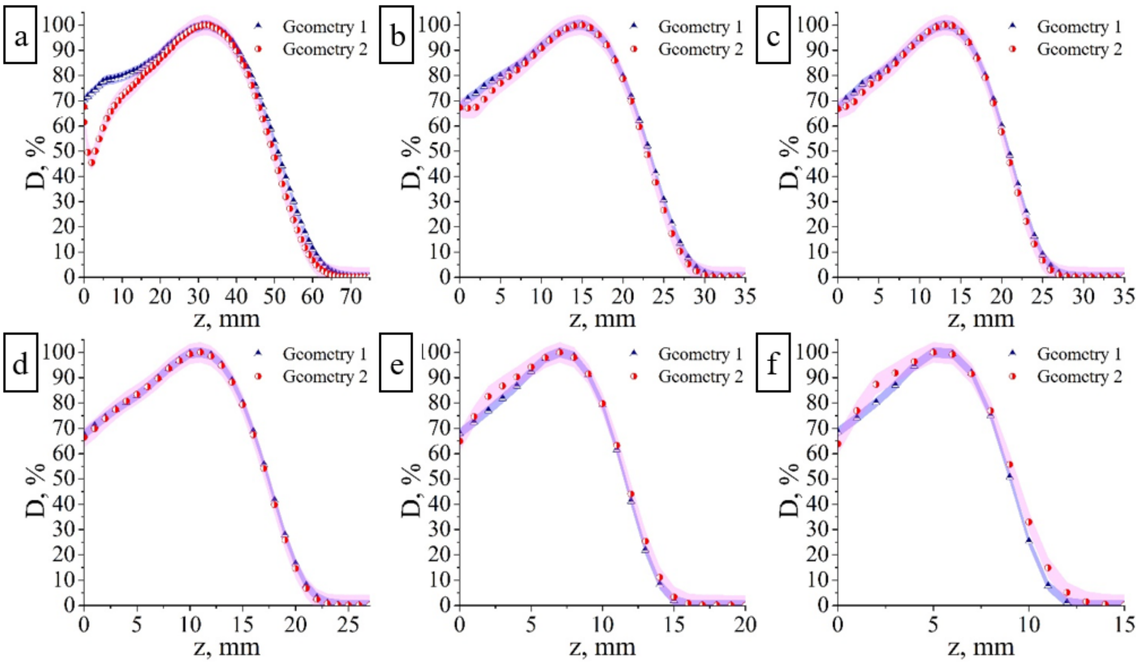

Figure 2. Simulated PDD in two geometries for different densities: a – 0.4 g/cm^3; b – 0.9 g/cm^3; c – 1.0 g/cm^3; d – 1.2 g/cm^3; e – 1.8 g/cm^3; f – 2.3 g/cm^3.

Table 1 shows the maximum range (R_{max}), half-value depth (R_{50}), therapeutic range (R_{90} – the depth of 90% value in PDD curve after the maximum absorption), the maximum difference of doses in the shallow depths (Δm), and the maximum difference of doses in the area that is deeper than the maximum absorption (ΔM) for certain densities (ρ). The table presents the values for two geometries without a film and with a film [14, 15].

Table 1. Main parameters of simulated PDD for certain media densities without/with a film.

ρ, g/cm^3	0.4	0.7	0.9	1.0	1.2	1.5	1.8	2.1	2.3
$R_{\max}$, mm	33/33	19/19	15/15	13/13	11/11	9/9	7/7	6/6	5/5
R_{50}, mm	51.5/50.5	29.7/29.3	23.1/22.9	20.8/20.6	17.3/17.3	14.8/14.9	11.6/11.7	9.8/10.1	9.0/9.3
R_{90}, mm	41.2/40.8	23.5/23.3	18.4/18.4	16.6/16.6	13.8/13.8	11.0/11.0	9.2/9.2	7y.8/7.8	7.2/7.2
Δm, %	27.66	12.08	5.46	3.66	1.24	4.54	5.55	6.87	7.24
ΔM, %	7.47	5.67	4.10	3.53	1.97	0.83	3.50	6.09	7.64

The coincidence of the PDD obtained in two geometries within the measurement accuracy (pink and blue areas in figure 2) is chosen as the data fitting criterion. As shown in the technical specification, the measurement accuracy of the Gafchromic EBT3 dosimetry film is about 4% [16]. For measurements without a film, the accuracy required by the dosimetry protocols is 2% when tissue-equivalent plates are used [14, 15]. For media densities ranging from 0.9 to 1.8 g/cm^3 (figure 2), the PDD in both geometries coincides within the predetermined error tolerance.

The difference in the PDD curves at shallow depths for low medium densities is caused by the more effective attenuation of the primary beam in a denser film material. At the same time, the contribution of scattered electrons from a denser medium causes the difference in the relative absorbed dose in the region of shallow depths for dense media.

The discrepancy in the region that is deeper than the absorption maximum for media with densities under 0.7 g/cm^3 is caused by deeper electron penetration into a homogeneous and less dense medium than in the case of a denser film. Contrariwise, the PDD difference in this region for dense media results from a deeper penetration of the radiation into the film.

The maximum range and therapeutic range in both geometries coincide for the calculated curves throughout the range under study. The half-value depth within the predetermined error rate coincides in both geometries for the medium densities ranging from 0.7 to 2.1 g/cm^3.

4 Summary

The PDD can be measured using tissue-equivalent dosimetry films with a longitudinal arrangement in media with densities from 0.9 to 1.8 g/cm^3. This result will simplify the experimental measurement of the PDD in the materials that are not tissue-equivalent but have densities close to that of water.

Moreover, this method can be used to determine the maximum range and therapeutic range for media with densities of 0.4 to 2.3 g/cm^3, and to measure the half-value depth for media with densities ranging from 0.7 to 2.1 g/cm^3, since they coincide within the predetermined tolerances in both geometries.

To determine the typical shape of the PDD curve in materials with densities under 0.9 g/cm^3 or over 1.8 g/cm^3, a different method should be used. It is based on measuring the dose at different depths using plates of the material under study with different thicknesses with the detector placed perpendicular to the beam axis.

Acknowledgments

This work is supported by the Russian Science Foundation (grant number 18-79-10052).

References

[1] A. Garibaldi, B.A. Jereczek-Fossa, G. Marvaso et al., *Recent advances in radiation oncology*, *Ecancer* **11** (2017) 785.

[2] D.W.O. Rogers, *Fifty years of Monte Carlo simulations for medical physics*, *Phys. Med. Biol.* **51** (2006) R287.

[3] A. Rodrigues, F.F. Yin and Q. Wu, *Dynamic electron arc radiotherapy (DEAR): a feasibility study*, *Phys. Med. Biol.* **59** (2013) 327.

[4] F.M. Khan and J.P. Gibbons, *Khan's the physics of radiation therapy*, Fifth edition, Lippincott Williams & Wilkins, Philadelphia, U.S.A. (2014), http://chopin.web.elte.hu/Khan.Phys_RT.pdf.

[5] S. Mueller, M.K. Fix, D. Henzen et al., *Electron beam collimation with a photon MLC for standard electron treatments*, *Phys. Med. Biol.* **63** (2018) 025017.

[6] http://www.parscientific.com/Acd4mk5.html.

[7] http://www.parscientific.com/Workstation.html.

[8] I. Miloichikova, A. Bulavskaya, Yu. Cherepennikov et al., *Feasibility of clinical electron beam formation using polymer materials produced by fused deposition modeling*, *Phys. Med.* **64** (2019) 188.

[9] M. Łukowiak, K. Jezierska, M. Boehlke et al., *Utilization of a 3D printer to fabricate boluses used for electron therapy of skin lesions of the eye canthi*, *J. Appl. Clin. Med. Phys.* **18** (2017) 76.

[10] I.A Miloichikova, A.A. Krasnykh, S.G. Stuchebrov et al., *Formation of electron beam fields with 3D printed filters*, *AIP Conf. Proc.* **1772** (2016) 060018.

[11] W. Zou, T. Fisher, M. Zhang et al., *Potential of 3D printing technologies for fabrication of electron bolus and proton compensators*, *J. Appl. Clin. Med. Phys.* **16** (2015) 90.

[12] C.Y. Liaw and M. Guvendiren, *Current and emerging applications of 3D printing in medicine.* *Biofabrication* **9** (2017) 024102.

[13] S. Su, K. Moran and J.L. Robar, *Design and production of 3D printed bolus for electron radiation therapy*, *J. Appl. Clin. Med. Phys.* **15** (2014) 194.

[14] P.R. Almond, P.J. Biggs, B.M. Coursey et al., *AAPM's TG-51 protocol for clinical reference dosimetry of high energy photon and electron beams*, *Med. Phys.* **26** (1999) 1847.

[15] P. Andreo et al., *Absorbed dose determination in external beam radiotherapy: an international Code of Practice for dosimetry based on standards of absorbed dose to water*, *IAEA Technical Reports Series no 398*, Vienna, (2000), https://www-pub.iaea.org/MTCD/publications/PDF/TRS398_scr.pdf.

[16] P. Sipilä, J. Ojala, S. Kaijaluoto et al., *Gafchromic EBT3 film dosimetry in electron beams energy dependence and improved film read-out*, *J. Appl. Clin. Med. Phys.* **17** (2016) 360.

[17] S. Devic, *Radiochromic film dosimetry: past, present, and future*, *Phys. Med.* **27** (2011) 122.

[18] M. Jaccard, K. Petersson, T. Buchillier et al., *High dose-per-pulse electron beam dosimetry: Usability and dose-rate independence of EBT3 Gafchromic films*, *Med. Phys.* **44** (2017) 725.

[19] N. Wen, S. Lu, J. Kim et al., *Precise film dosimetry for stereotactic radiosurgery and stereotactic body radiotherapy quality assurance using Gafchromic™ EBT3 films*, *Radiat. Oncol.* **11** (2016) 132.

[20] L. Campajola, P. Casolaro and F. Di Capua, *Absolute dose calibration of EBT3 Gafchromic films*, 2017 *JINST* **12** P08015.

[21] M. Severgnini, M. de Denaro, M. Bortul et al., *In vivo dosimetry and shielding disk alignment verification by EBT3 GAFCHROMIC film in breast IOERT treatment*, *J. Appl. Clin. Med. Phys.* **16** (2015) 112.

[22] R. Abedi Firouzjah, A. Nickfarjam, M. Bakhshandeh et al., *The use of EBT3 film and Delta4 for the dosimetric verification of EclipseTM treatment planning system in a heterogeneous chest phantom: an IMRT technique*, *Int. J. Radiat. Res.* **17** (2019) 355.

[23] W. Crijns, G. Defraene, H. Van Herck et al., *Potential benefits of dosimetric VMAT tracking verified with 3D film measurements*, *Med. Phys.* **43** (2016) 2162.

[24] C.M.C. Ma, I.J. Chetty, J. Deng et al., *Beam modeling and beam model commissioning for Monte Carlo dose calculation-based radiation therapy treatment planning: Report of AAPM Task Group 157*, *Med. Phys.* **47** (2019) e1.

[25] I.A. Miloichikova, B.M. Gavrikov, A.A. Krasnykh et al., *Numerical Model Simulating the Therapeutic Electron Beam of a Clinical Linear Accelerator*, *Biomed. Eng.* **53** (2020) 345.

[26] D. Henzen, P. Manser, D. Frei et al., *Monte Carlo based beam model using a photon MLC for modulated electron radiotherapy*, *Med. Phys.* **41** (2014) 021714.

[27] I.A. Miloichikova, S.G. Stuchebrov, I.B. Danilova et al., *Simulation of the microtron electron beam profile formation using flattening filters*, *Phys. Part. Nucl. Lett.* **13** (2016) 890.

[28] I.A. Miloichikova, V.I. Bespalov, A.A. Krasnykh et al., *Analysis of Plane-Parallel Electron Beam Propagation in Different Media by Numerical Simulation Methods*, *Russ. Phys. J.* **60** (2018) 2115.

[29] http://portal.tpu.ru/SHARED/b/BVI/eng/PCLab.

[30] V.I. Bespalov, *EPHCA software package for statistical modeling of the radiation field of photons and charged particles* (in Russian), *Russ. Phys. J.* **43** (2000) 159.

[31] http://www.siemens.com.tr/i/assets/saglik/onkoloji/oncor.pdf.

[32] https://bitfab.io/blog/3d-printing-materials-densities/.

[33] http://www.gafchromic.com/documents/EBT3_Specifications.pdf.

2020 JINST 15 C03037